NATIONAL TRANSPORTATION SAFETY BOARD
Office of Research and Engineering
Materials Laboratory Division
Washington, D.C. 20594

April 8, 2020

MATERIALS LABORATORY FACTUAL REPORT Report No. 20-010

1. ACCIDENT INFORMATION

Place	:	Newmarket, Virginia
Date	:	December 15, 2019
Vehicle	:	Piper PA-18A, N1984A
NTSB No.	:	ERA20LA055
Investigator	:	Brian Rayner, AS-ERA

2. COMPONENTS EXAMINED

Remnants of a landing gear dampener
Fragments of a landing gear leg

3. DETAILS OF THE EXAMINATION

Several pieces from a landing gear installed on a Piper PA-18A were sent to the NTSB Materials Laboratory after it was involved in an accident during landing in Newmarket, VA on December 15, 2019. These included portions of a dampener assembly, pieces of a landing gear arm, and pieces of a rubber cover.

Figure 1 shows the parts from the dampener assembly, as received. This assembly consisted of a dampening piston system, contained inside a housing, and a piston rod. The rod had fractured at a thread root, as annotated in Figure 1. The markings on the side of the rod stated, “BAR 18-9A-11.6 FAA-PMA”. The housing of the dampener exhibited inward denting and buckling, as exemplified in Figure 2. This damage was consistent with an impact with an adjacent component or a ground object.

The piston rod to the dampener had fractured along a thread root next to the hexagonal collar. The markings on the side of the rod stated, “LEFT HAND, MAX THREAD, ½” FROM NUT.” Figure 3 shows the mating sides of the fracture surface, from the dampener side and the rod side. The rod side fracture surface was sectioned away from the rod for closer examination.

Figure 4 shows the rod side fracture surface, viewed with direct and oblique lighting. The fracture surface exhibited a rough, tortuous texture and a dull, gray luster. There were river patterns that were consistent with fracture from one side of the rod towards the other. Figure 4 is annotated to show this general fracture direction, from the lower side in the

figure towards the upper side. The upper side exhibited smoother and shinier regions locally. These shiny features were consistent with smearing, a type of post-fracture damage on this section of the fracture surface.

The initial regions of the rod fracture are shown closer in Figure 5. As shown in the figure, river pattern features were consistent with fracture beginning at a thread root on the rod surface. The fracture surface was examined using a scanning electron microscope (SEM). Figure 6 shows a general view of this initial side of the fracture surface. The darker areas were consistent with non-conductive material, typical of post-fracture contamination of the surface. An area of the fracture surface that was not contaminated (yellow box in Figure 6) region was examined closer, as illustrated in Figure 7. The fracture features in this region were typical of the rest of the fracture surface. This region exhibited dimpled rupture, consistent with overstress fracture.

The opposite end of the fracture surface is shown in Figure 8. This area had been damaged by post-fracture smearing. The undamaged areas were examined closer, as typified in Figure 9. These fracture features, exhibiting dimpled rupture, were consistent with overstress fracture. No indications of pre-existing fracture features, such as corrosion or fatigue striations, were found. The fracture features of the rod were consistent with a tensile overstress and bending in the direction depicted in Figure 4.

The chemical composition of the rod was inspected using energy dispersive x-ray spectroscopy (EDS). The chemical composition was consistent with a Ti-6Al-4V titanium alloy. The hardness of the dampener piston rod was tested per ASTM E18.[1] The hardness of the piston rod averaged 30 HRC. This hardness was typical for this alloy.

The mating fragments of the landing gear arm are shown in Figures 10 and 11, placed in their approximate respective positions at the time of the fracture. As shown in Figure 11, there was a faint red paint stripe along the length of the cylindrical tube portion of the arm. This and other markings were used to position the fragments near their mating positions.

As shown in closer views in Figures 12 and 13, the fractured sides only mated along a small, 0.5-inch, portion of the fracture surface. This was consistent with another fractured piece or pieces of the arm assembly which were not received by the Materials Laboratory.

Besides the fracture, other damage was noted on the arm assembly fragments. Much of the paint near the fracture exhibited spalling and cracking. There were indications of sliding and impact marks, such as shown in Figure 14.

Figure 15 through 17 show closer views of the mating fracture surfaces of the arm. These fracture surfaces exhibited a general 45° slanted orientation, except on one section that protruded outward. This protrusion exhibited localized thinning, or necking, of material adjacent to the fracture surface. The paint in this area had fractured, and the orientation

[1] ASTM E18 – *Standard Test Methods for Rockwell Hardness and Rockwell Superficial Hardness of Metallic Materials*. ASTM International, West Conshohocken, PA.

of the cracked lines in the paint was consistent with having originated from the fracture surface—these cracked lines branched out running away from the fracture.

The fracture surface exhibited a dull luster and rough texture. In general, the fracture surface exhibited river patterns that were consistent with fracture from the lower slanted sides toward the elongated and necked side. All these features were consistent with the arm having fractured from overstress, in the direction as annotated in Figure 17. There were no indications of pre-existing defects or cracking in the arm. The fracture pattern was consistent with overstress fracture in tension, which then also bent outward at the end of the fracture (right side of Figure 17).

In addition, some internal features were present next to the fracture surface on a portion the arm. These were consistent with the interior surface finish being damaged from the fracture and localized necking of the arm.

The chemical composition of the arm was inspected using x-ray fluorescence (XRF). The chemical composition was consistent with a 4130 steel.

A small protruding red rubber cover was also submitted, as depicted in Figure 18. The cover had fractured about the fitting hole, as shown in Figure 18b. This piece exhibited an orangish-red color, and had cracked or split from the rectangular hole on the mating end.

Erik M Mueller
Materials Research Engineer

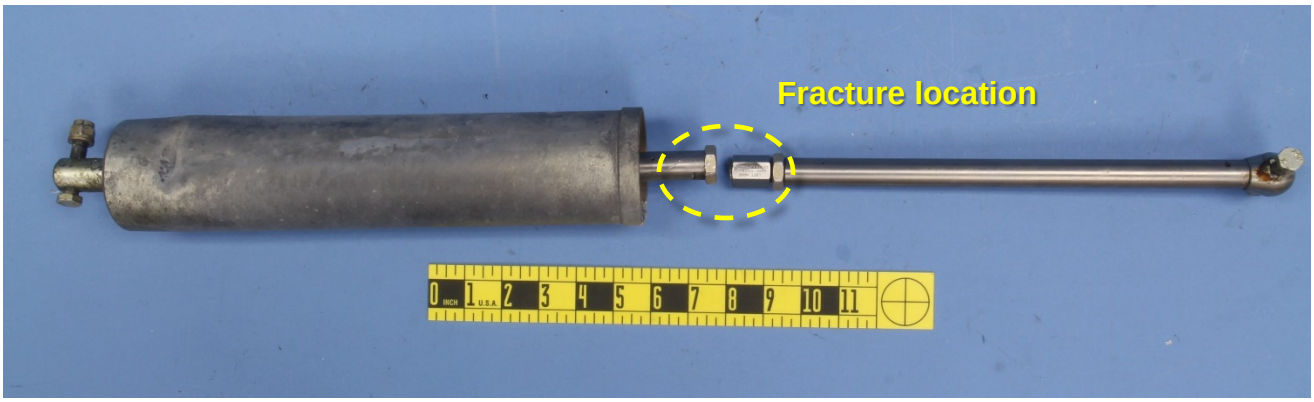

Figure 1 – Fractured dampener assembly, as received. The piston had fractured at the circled location.

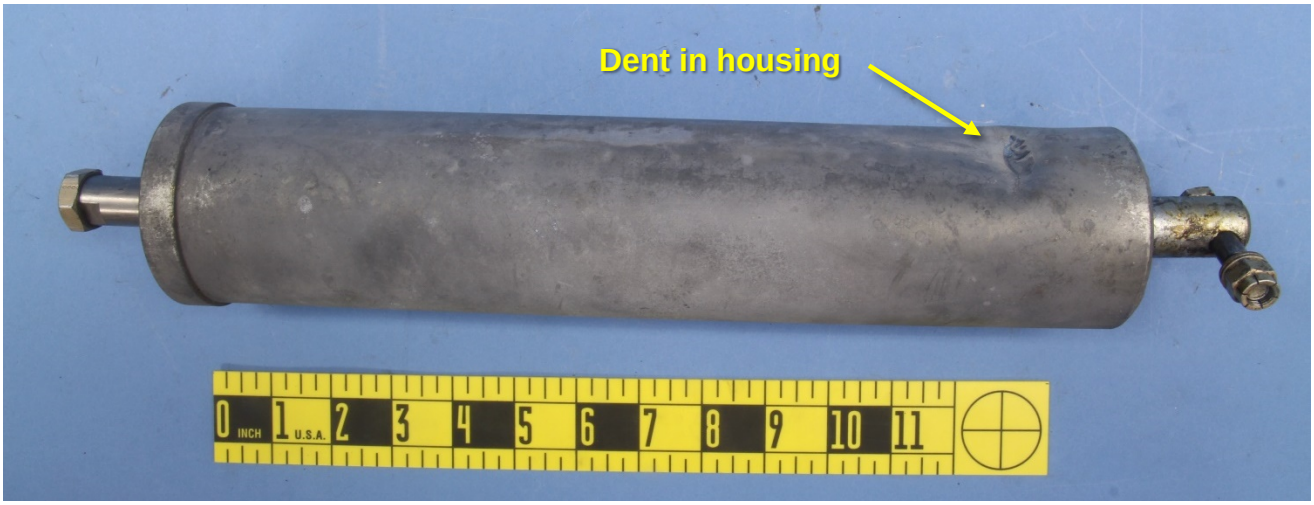

Figure 2 – Closer view of the dampener housing showing a dent in the surface opposite the fracture region (left side).

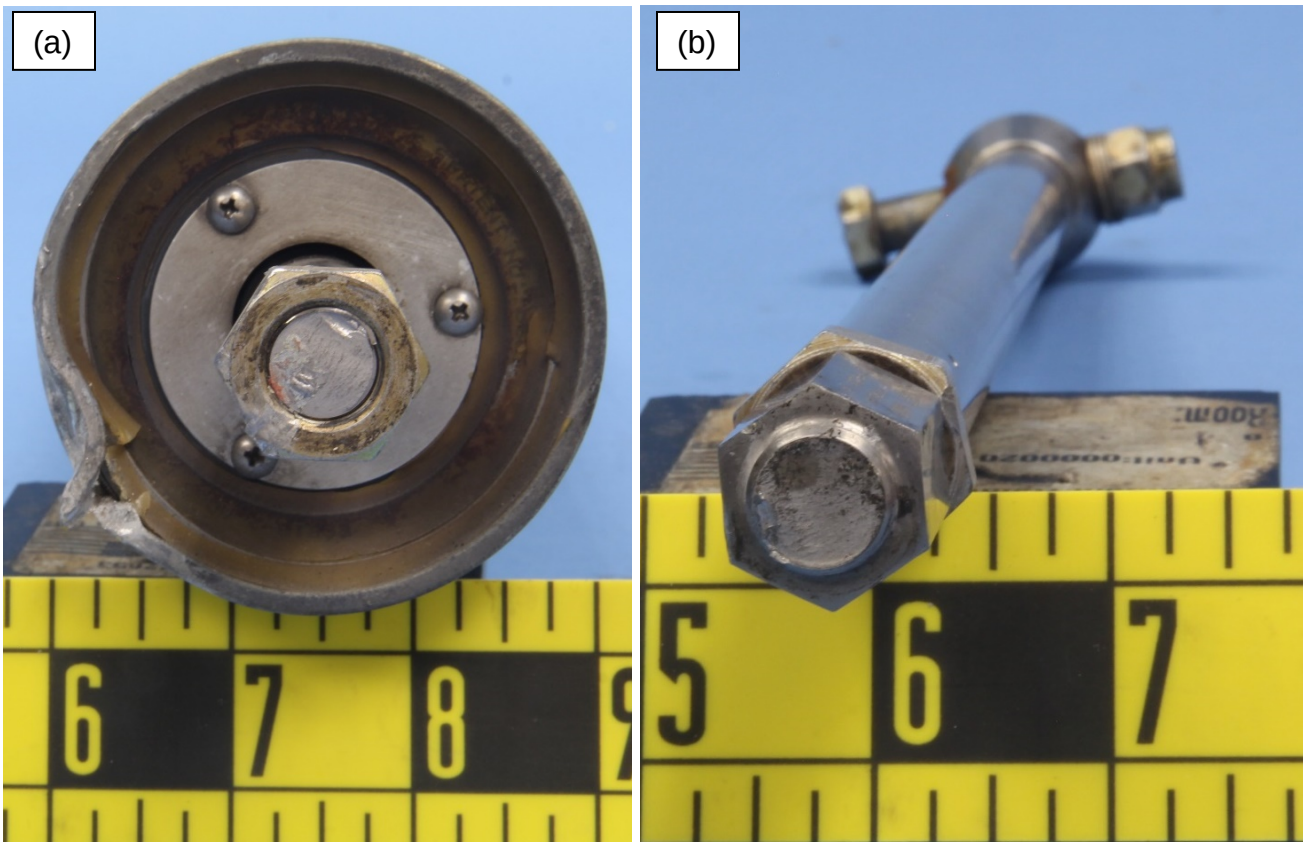

Figure 3 – Fracture surface of the dampener piston from (a) the assembly side and (b) the piston rod side.

Figure 4 – Closer view of the rod side fracture surface from Figure 3b. The arrows denote the general fracture direction.

Figure 5 – Closer view of the lower portion of Figure 4, showing the the region the fracture originated.

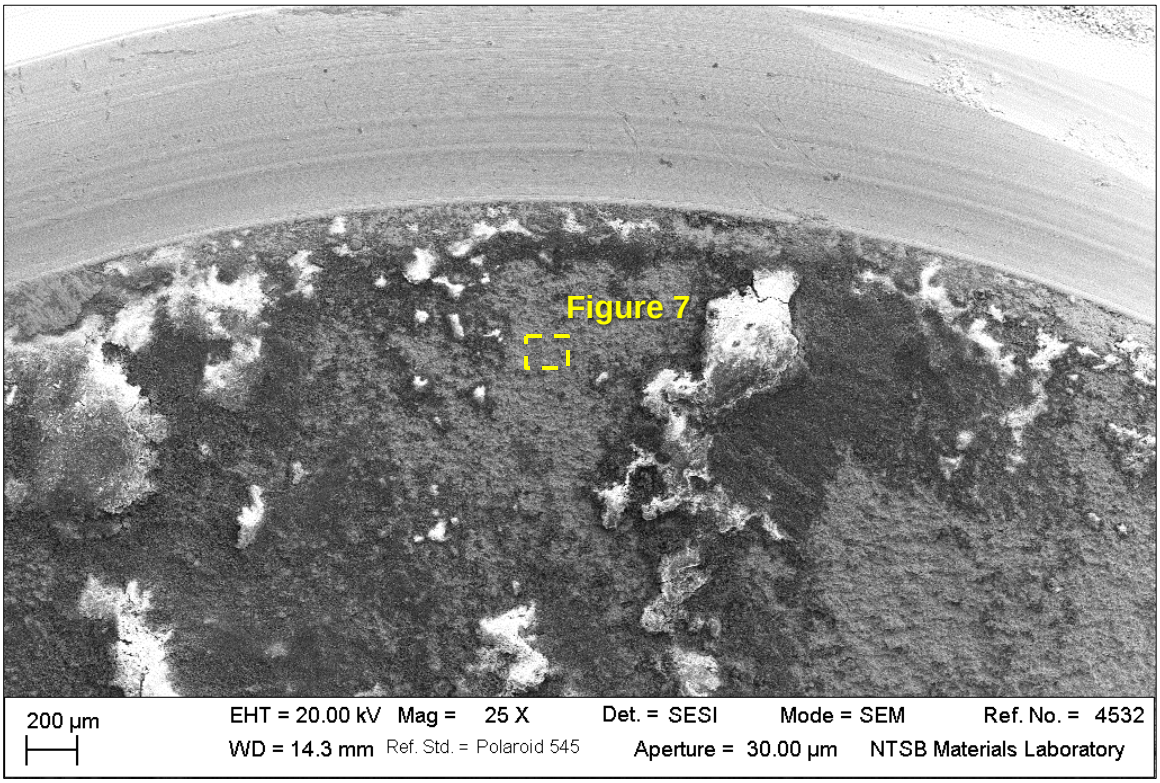

Figure 6 – Secondary electron (SE) micrograph of the fracture initiation area on the dampener rod fracture (viewed reversed from Figure 5).

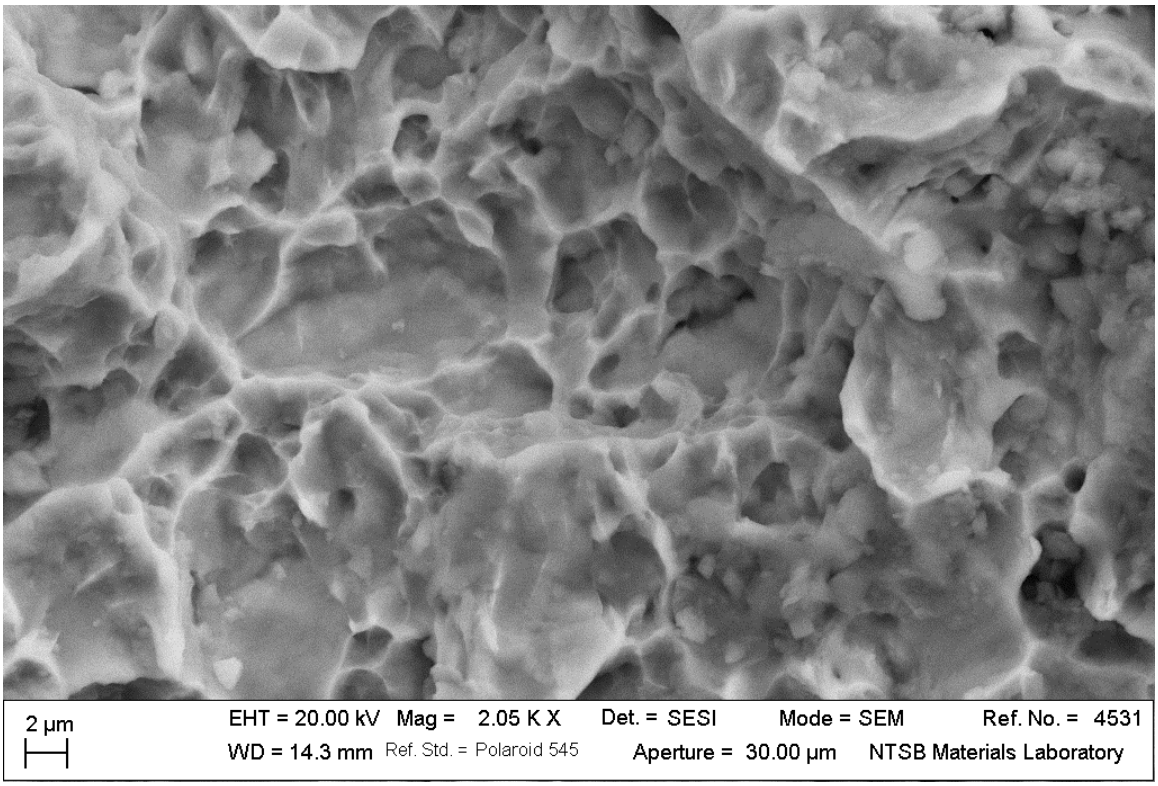

Figure 7 – SE micrograph of dimpled rupture on the boxed area in Figure 6.

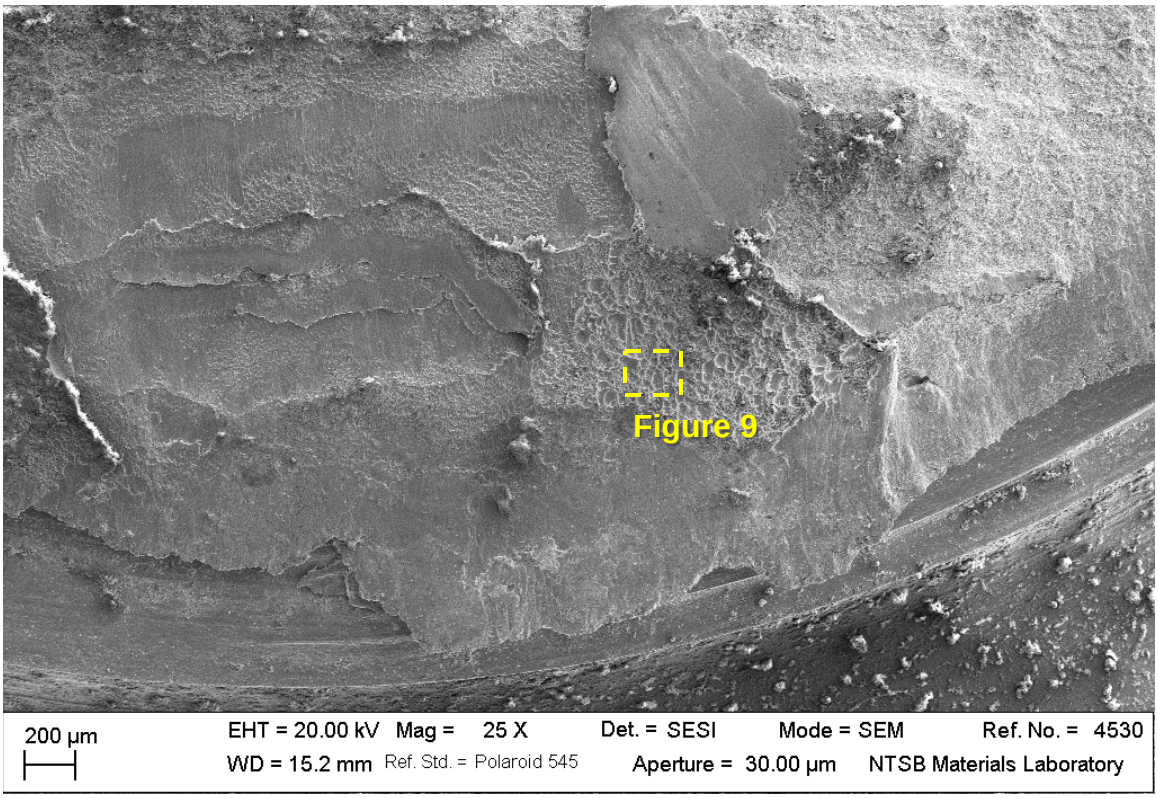

Figure 8 – SE micrograph of the smeared area on the top of Figure 4.

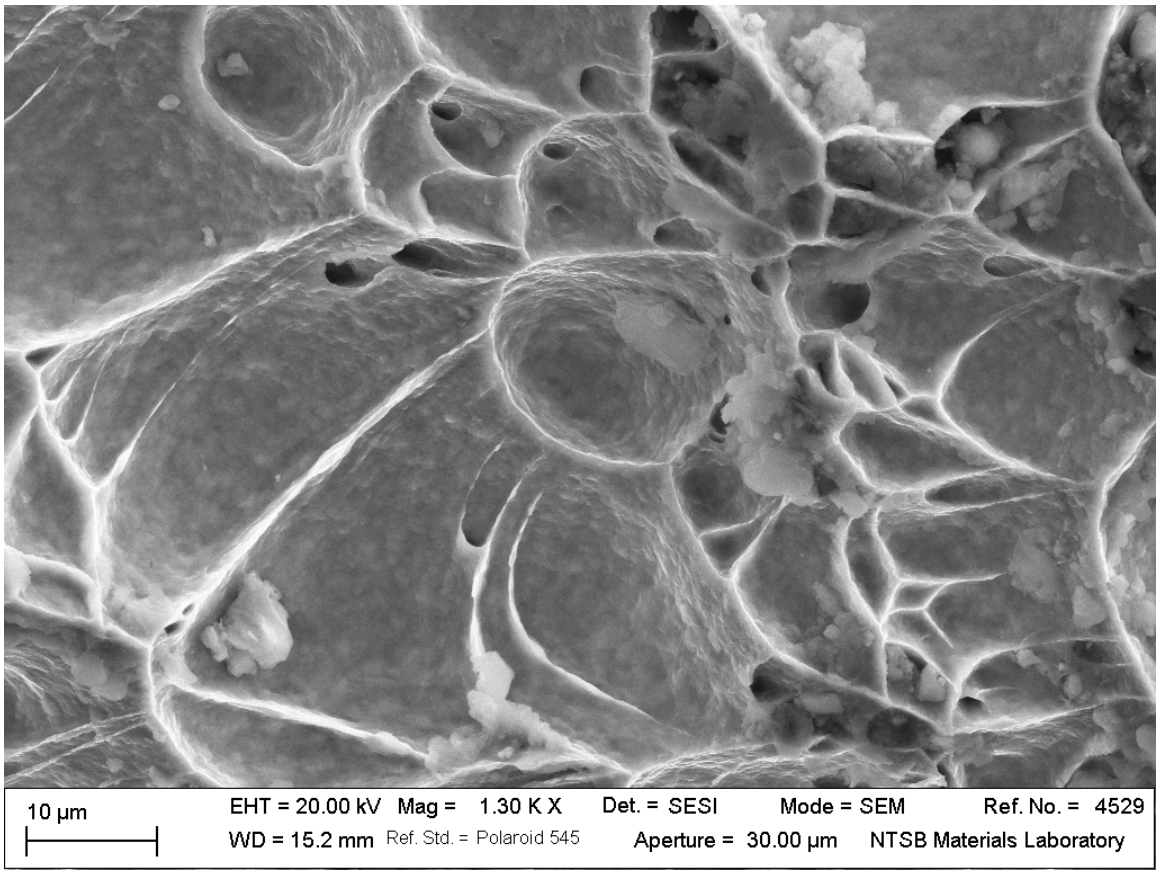

Figure 9 – SE micrograph of dimpled rupture from the boxed area in Figure 8.

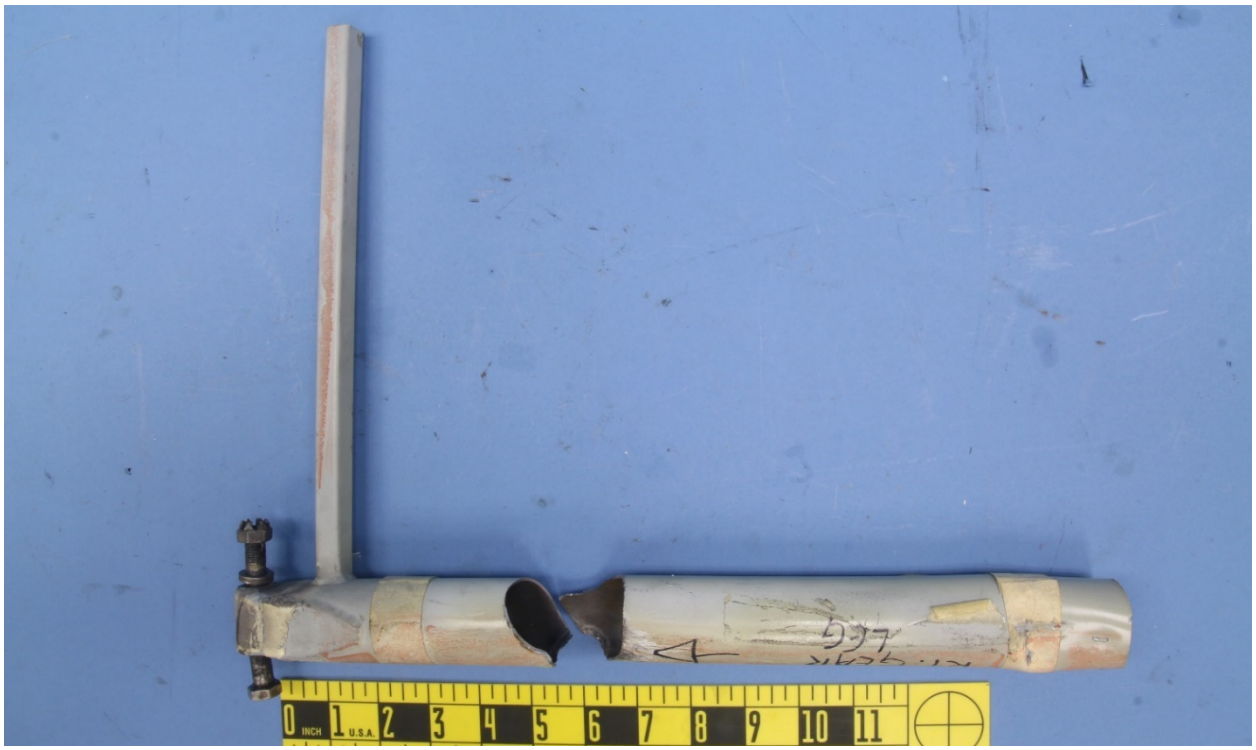

Figure 10 – The fragments of the landing gear arm, positioned near their pre-fracture places.

Figure 11 – The repositioned landing gear arm fragments, shown opposite those in Figure 10.

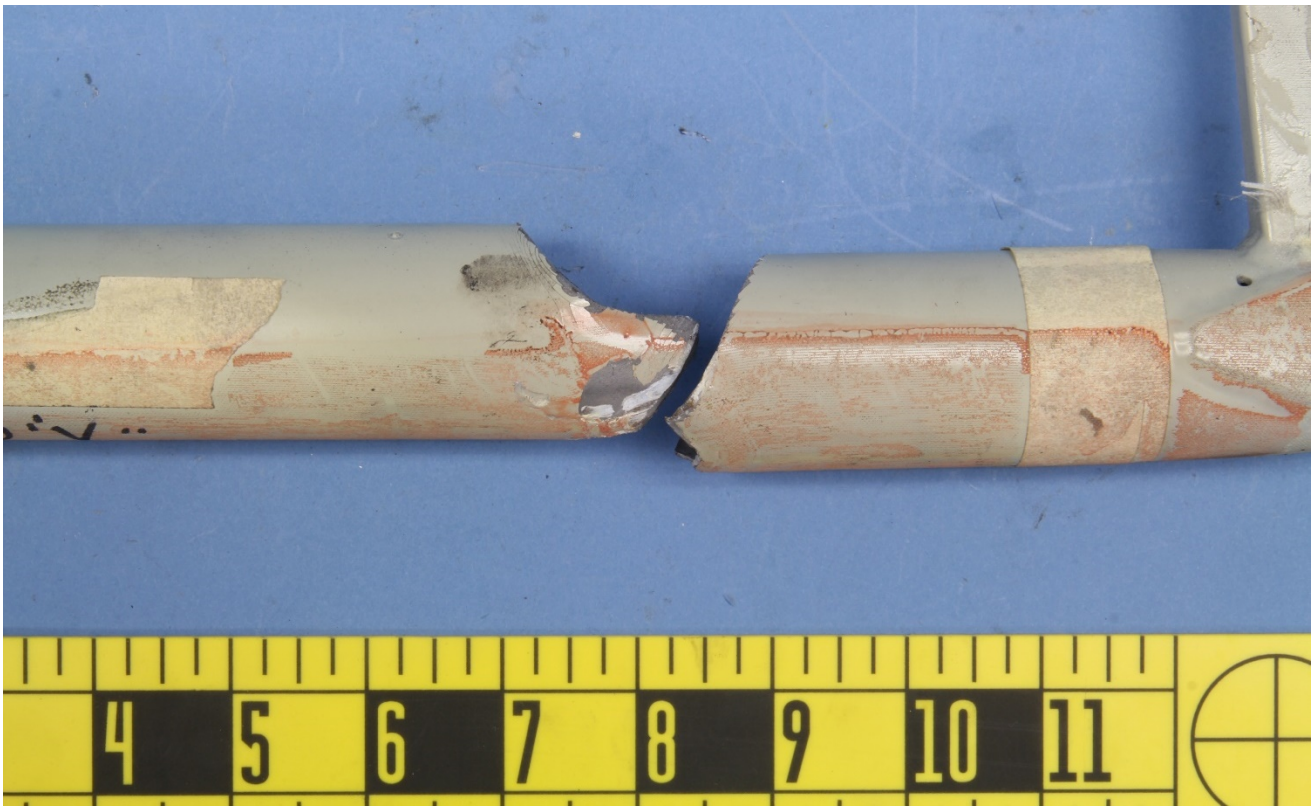

Figure 12 – The mating fracture surfaces of the arm fragments, viewed from the outer surface.

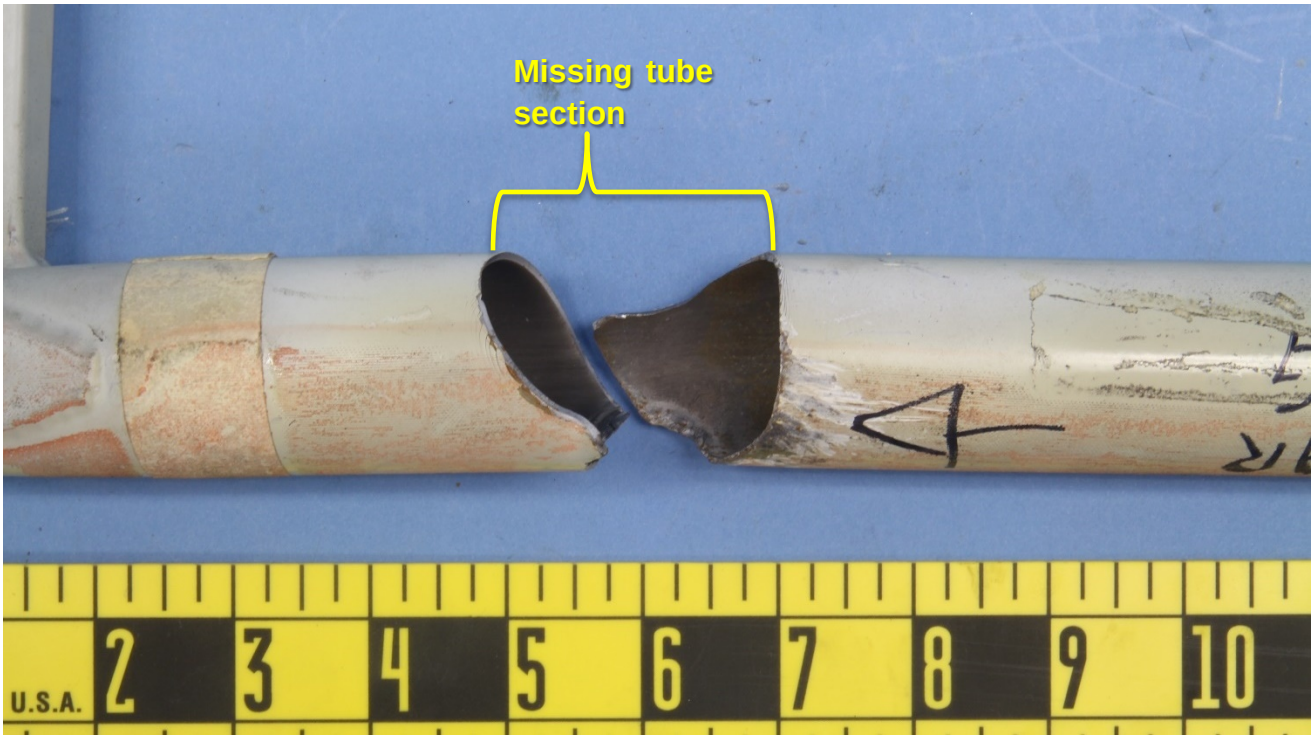

Figure 13 – The mating arm fractures, viewed opposite Figure 12 from inside, showing the missing material.

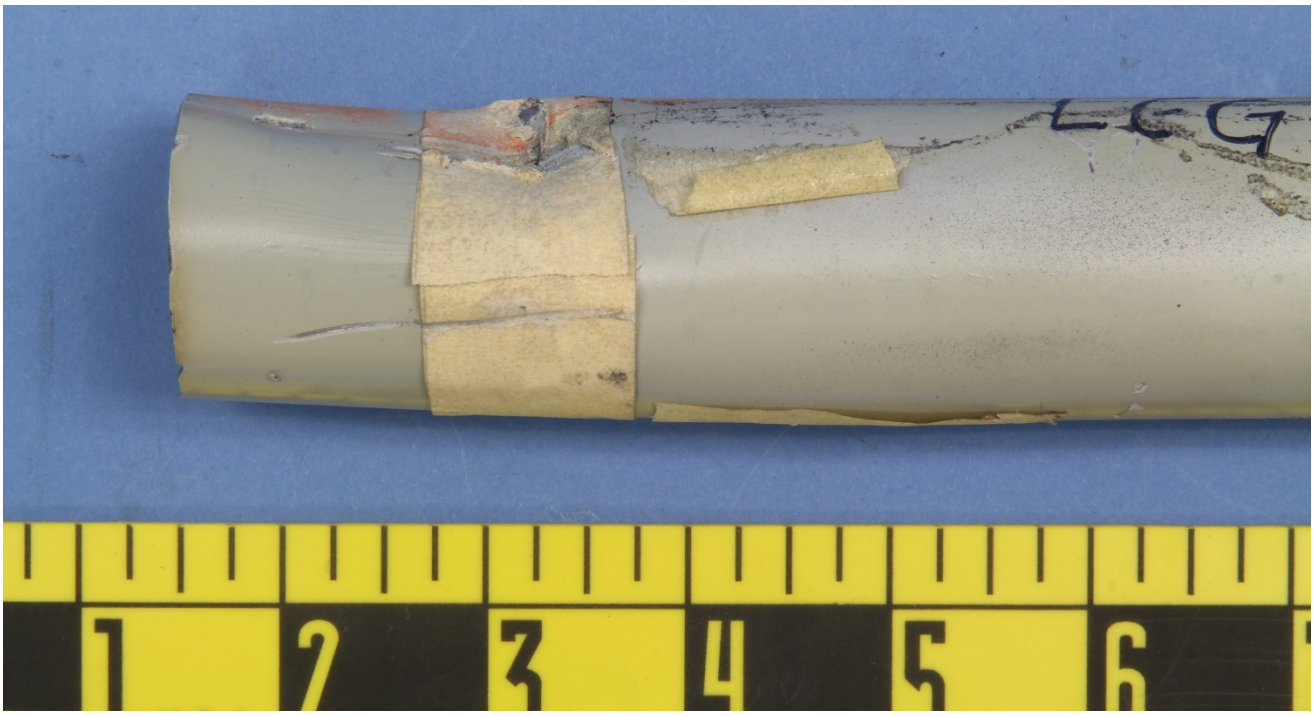

Figure 14 – A dent in one of the arm fragment near a sectioned portion.

Figure 15 – Closer view of the inner surface of the right arm fragment in Figure 13.

Figure 16 – Closer view of the outer surface of the right arm fragment in Figure 13.

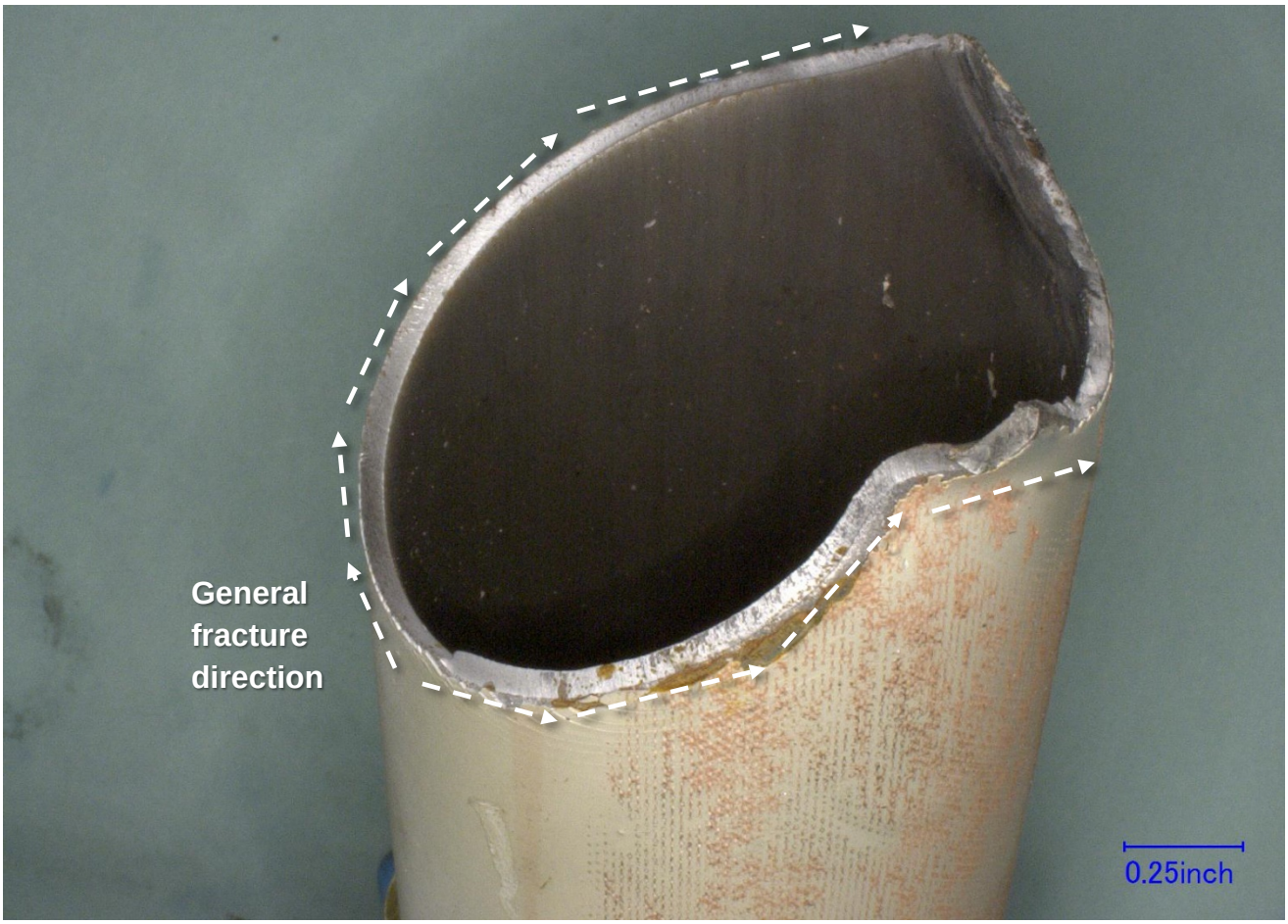

Figure 17 – View of the fracture surface of the left arm fragment in Figure 13, annotated to show the general fracture direction.

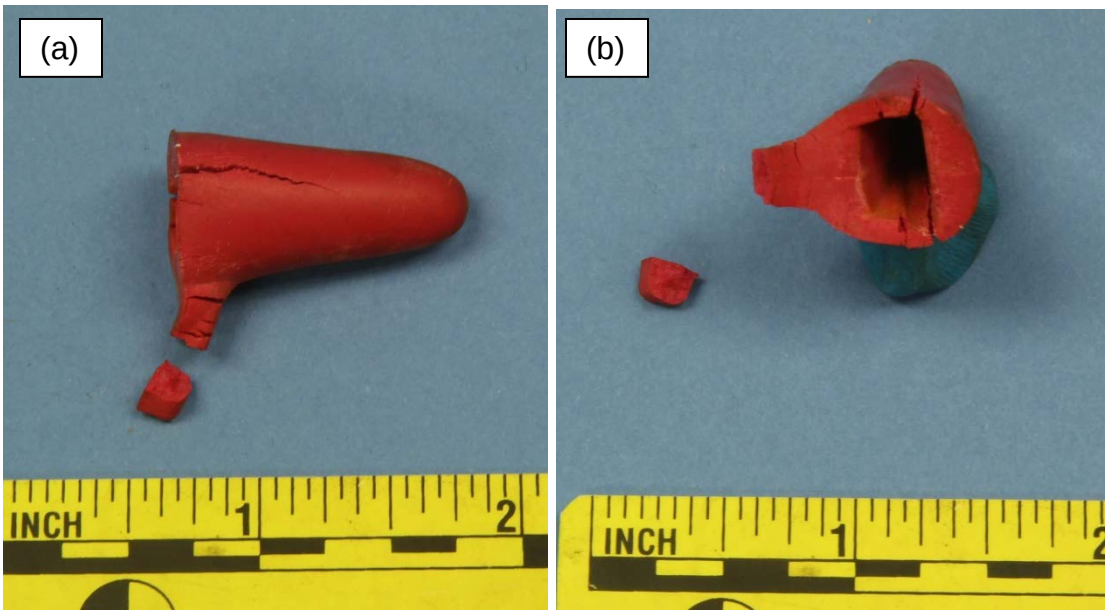

Figure 18 – View of the rubber cover from (a) the side and (b) the mating end.